11 Optical Coherence Tomography: Emerging In Vivo Optical Biopsy Technique for Oral Cancers

Prashanth Panta, Chih-Wei Lu, Piyush Kumar, Tuan-Shu Ho, Sheng-Lung Huang, Pawan Kumar, C. Murali Krishna, K. Divakar Rao, and Renu John

Abstract

Oral cancers are a major health burden, and patients suffer from low survival rate owing to their late detection. Optical techniques are rapid, objective, and noninvasive methods with the potential to serve as adjunct screening/diagnostic tools, especially for cancers. This chapter highlights the advancements in oral cancer exploration using optical coherence tomography (OCT) with a discussion on basic principles of OCT, followed by a detailed description of oral cancer studies, subgrouped into animal studies, and ex vivo and in vivo human studies. We have included full-field OCT system-derived in vivo oral mucosa images in a healthy volunteer at different subsites showing standard microanatomy at various depths and also narrated some strategies to improve OCT results by multimodal approaches as well as through contrast enhancement for improved visualization.

11.1 Introduction

Optical coherence tomography (OCT) is a widely explored imaging modality that can provide high-resolution, cross-sectional tomographic images of the ultrastructure of biological samples. OCT applications were reported in the early 1990s for noninvasive imaging of the retina [1, 2], and owing to its numerous advantages, it has been explored in a range of biomedical applications

P. Panta, MDS (✉)
Department of Oral Medicine and Radiology,
MNR Dental College and Hospital,
Sangareddy, Telangana, India
e-mail: maithreya.prashanth@gmail.com

C.-W. Lu, PhD
Apollo Medical Optics, Ltd. (AMO), Taipei, Taiwan
e-mail: cwlu@mdamo.com

P. Kumar, PhD
Amity Institute of Biotechnology,
Amity University Mumbai, Navi Mumbai,
Maharashtra, India

T.-S. Ho, PhD · S.-L. Huang, PhD
Apollo Medical Optics, Ltd. (AMO), Taipei, Taiwan

Graduate Institute of Photonics and Optoelectronics,
National Taiwan University, Taipei, Taiwan

P. Kumar · R. John, PhD
Department of Biomedical Engineering,
Indian Institute of Technology, Hyderabad,
Telangana, India
e-mail: renujohn@iith.ac.in

C. Murali Krishna, PhD
Chilakapati Laboratory,
Advanced Centre for Treatment Research and
Education in Cancer (ACTREC), Tata Memorial
Centre (TMC), Mumbai,
Maharashtra, India

Homi Bhabha National Institute,
Anushakti Nagar, Mumbai, India

K. Divakar Rao, PhD
Photonics and Nanotechnology Section,
Bhabha Atomic Research Centre Facility,
Visakhapatnam, India

P. Panta (ed.), *Oral Cancer Detection*, https://doi.org/10.1007/978-3-319-61255-3_11

including ophthalmology [3, 4], oncology [5–7], cardiology [8], and developmental biology [9]. OCT became a tool of choice for cancer researchers due to the feasibility of noninvasive high-resolution functional imaging and tumor margin assessment and has been extensively explored in skin cancers [10–12], laryngeal cancers [13], esophageal cancers [14–17], cervical cancers [18], bladder cancers [19], and oral cancers [20–22]. Oral cancers have become a global burden, especially in the developing nations of Southeast Asia [23]. Despite advancements in treatment approaches, the survival rate is dismal particularly due to late detection, often at stages III–IV at time of diagnosis. Optical techniques, like OCT, have thus become an important tool to serve as a powerful diagnostic adjunct to clinical examination. In this chapter we will summarize the developments in the field of OCT and discuss its applications for oral cancers.

11.1.1 Basis for OCT

While histology utilizes thin tissue sections (~5 μm) stained to highlight salient features, OCT generates cross-sectional images (similar to microtome sectioning) from light backscattered through tissues, typically without the need for any staining methods. OCT can be understood as an optical analog of ultrasound imaging which measures backscattered intensity of light instead of sound. It is noteworthy that histology and OCT images correspond well and thus can be used for appropriate clinical correlation. Cancer progression disrupts tissue architectural arrangement leading to a change in the intensity of backscattered light. OCT images can thus be used for noninvasive, real-time imaging to obtain cross-sectional as well as three-dimensional images.

11.2 Instrumentation

11.2.1 Working Principle

OCT is an interferometry-based imaging technique that uses near-infrared (NIR) light to map the depth-wise reflections from tissue to form cross-sectional images of morphological features at the scale of a micrometer. Huang et al. used OCT to obtain two-dimensional images based on the optical scattering of microstructures within the retina. Since then, several adaptations of OCT have been developed. A typical setup for OCT would consist of a low-coherence light source, a lateral-scanning mechanism, and an optical interferometer (Fig. 11.1). The Michelson interferometer splits the light into sample arm and reference arm and recombines the backscattering signal

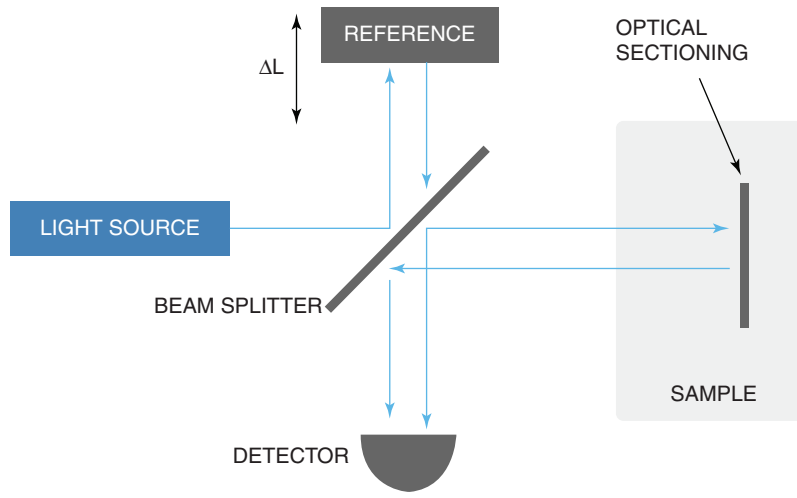

Fig. 11.1 Schematic showing optical sectioning of sample (ΔL, change of optical path length)

with the reflected reference light to a photodetector. OCT originated from optical coherence-domain reflectometry and rapidly gained value for biological applications [24, 25]. The spatial resolution of modern OCT systems is ~1–15 μm, and the imaging depth in scattering tissues is around 1–3 mm [26, 27]. Axial resolution of 10 μm is commonly employed, whereas ultrahigh axial resolution of ~1 μm has been achieved with a photonic crystal fiber [28]. Usually light source includes a low-coherence length source that can be generated by a superluminescent diode or an ultrafast (titanium-sapphire) laser (Fig. 11.2a–c). Incident signal is passed through a fiber coupler which is split into a sample arm and reference arm of the interferometer. Light reflected from sample is collected by sample arm fiber, and light reflected by reference mirror is collected by reference arm fiber. Reflected light from both arms is once again passed through the coupler and split into two parts where it is redirected toward the detector to form an interference pattern. The interference pattern is visible only when the optical path difference between the two arms is less

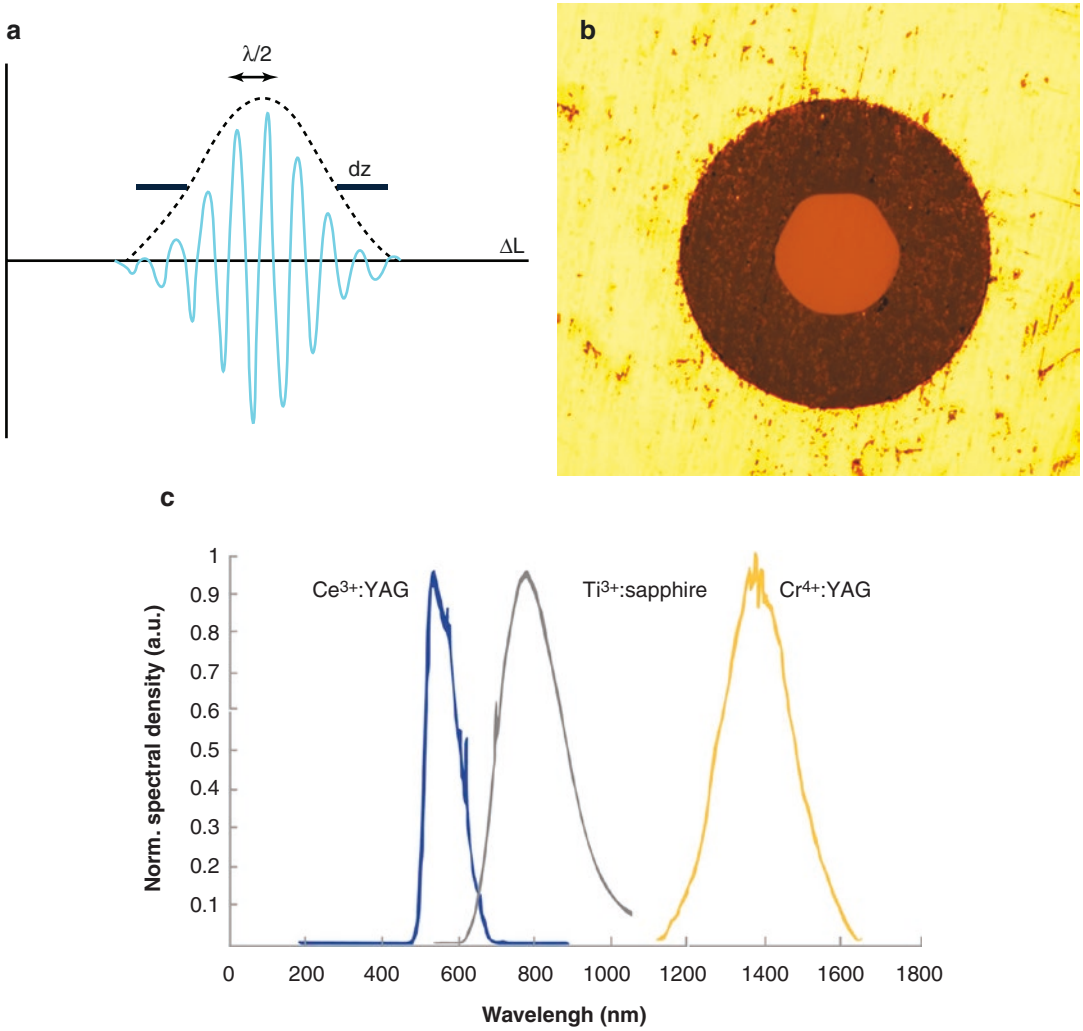

Fig. 11.2 Panel (**a**) shows the low-coherence length in OCT imaging characteristic of shorter center wavelength and broader bandwidth (λ, center wavelength of light source; dz, coherence length; ΔL, change of optical path length); panel (**b**) shows the crystalline fiber core cross section; and panel (**c**) compares spectral densities of different crystal-based light sources

than the coherence length of the light source. Since coherence length is inversely proportional to the optical bandwidth of the light source, OCT integrated with broadband low-coherence light source is able to discriminate closely adjacent signals and produces high-resolution image. In the recent times, imaging is being performed using a scanned optical beam from surgical microscopes, through user-friendly handheld probes and minimally invasive needle-biopsy probes.

11.2.2 Adaptation of OCT

Depending on the signal detection mechanism and data processing algorithms, OCT is classified as either time domain OCT (TD-OCT) or Fourier domain OCT (FD-OCT). FD-OCT can be further categorized into spectral domain OCT (SD-OCT) and swept-source OCT (SS-OCT). Other improvements on OCT include polarization-sensitive OCT, which detects changes in the polarization state of reflected light [29].

TD-OCT was the first generation of OCT, where the reference mirror is mounted on a moving stage and the depth profile is recorded by shifting the mirror linearly. As mechanical movement is involved in TD-OCT, it is restricted to a slow imaging speed, thereby limiting its biomedical application. In SD-OCT, the reference arm does not move, and depth-resolved structural information is extracted by capturing the interference spectrum in a spectrometer. In the case of SS-OCT, depth information of the sample is extracted by sweeping the individual wavelength spectrum emitted from a broadband source. Consequently, SS-OCT is also called optical frequency-domain imaging (OFDI). An advantage of the FD-OCT methods is higher signal to noise ratio and faster acquisition speed in comparison to TD-OCT. Furthermore, with SS-OCT, higher image acquisition rate and longer depth of imaging are achieved in comparison to SD-OCT. OCT techniques can also be combined with optical coherence microscopy (OCM) for confocal imaging. OCT combined with optical Doppler tomography (ODT) has been used for early diagnosis as well as evaluation of chemotherapy-induced oral mucositis and is capable of providing information about functional activity in tissue such as tissue blood flow. PS-OCT measures reflected both light intensity and the polarization state of the light signal coming from the sample. As such, PS-OCT can provide higher contrast between normal tissue and diseased tissue.

11.3 Biological Applications: OCT in Oral Cancers

OCT can be used both as an ex vivo and in vivo diagnostic tool and provides information on architectural changes or disorganized orientation and can discern epithelial pathology in oral tissues. Gross histological features suggestive of oral squamous cell carcinoma (OSCC) that can be detected with OCT include enlarged nuclei, increased nuclear-cytoplasmic ratio, altered rete peg organization, and discontinuity in basement membrane, which are common cellular and tissue alterations. The last two decades have witnessed OCT taking a major stride in oral cancer detections, leading to advancement in the field of novel diagnostic tools. In this chapter, we systematically discuss the topic by broadly classifying oral cancer studies into animal studies, ex vivo studies on human tissues, and in vivo clinical studies (Table 11.1).

11.3.1 Animal Studies

There are several exploratory OCT studies which have employed animal models of oral cancers [30–35]. A commonly used animal model is the hamster buccal pouch (HBP) model, already elaborated in the Chapter titled “Optical techniques: Investigations in Oral Cancers” in this book and also in these references [36, 37]. Briefly, HBP model forms tumors in 14 weeks, progressing through stages like hyperplasia,

Table 11.1 Summary of landmark studies on optical coherence tomography application for oral cancers, oral potentially malignant conditions, and healthy oral mucosa

Author	Year	Study type	Findings
Feldchetein et al	1998	First in vivo study	In vivo OCT imaging differentiates keratinized and nonkeratinized mucosa with high resolution [48]
Petra Wilder-Smith et al.	2004	Hamster pouch	Epithelial and subepithelial changes were recorded in hamster pouch model ($n = 32$). Agreement of OCT diagnosis and histopathology was 80% [34]
Matheny et al.	2004	Hamster pouch	OCT and optical Doppler tomography (ODT) combination detected vascular changes in hamster cheek pouch ($n = 22$). Good resolution was obtained to depth of 1–3 mm [30]
Petra Wilder-Smith et al.	2005	Hamster pouch	Specific application of OCT and ODT in hamster pouch ($n = 120$) and also in vivo multi-wavelength multiphoton (MPM) and second harmonic-generated (SHG) fluorescence as promising noninvasive modalities [21]
Hanna et al.	2006	Hamster pouch	OCT offered exceptional cheek pouch depth (1–3 mm), and 3D construction was possible for visualizing extent and tumor margins [31]
Ridgway et al.	2006	In vivo	OCT images of normal oral cavity ($n = 41$ patients) and pathological changes (leukoplakia, invasive cancer, etc.) were obtained [50]
Tsai et al.	2008	Ex vivo (SS-OCT)	First use of swept-source OCT for ex vivo oral lesion delineation, particular value in the determination of margins [39]
	2009	In vivo	Differentiating oral lesions based on carcinogenic stage of lesion using a SS-OCT system was possible because well-differentiated SCC had higher tissue absorption and decay constants [22]
Petra Wilder-Smith et al.	2009	In vivo	OCT showed excellent in vivo capability (i.e., histopathology agreement) in oral malignancy/premalignancy diagnosis ($n = 50$ lesions) [21]
Kim et al.	2009	First contrast enhancement attempt in hamster model	Contrast enhancement in OCT using surface plasmon resonant gold nanoparticles via microneedle and ultrasound-assisted delivery [82]
Park et al.	2010	Hamster pouch	Dual modality of OCT and FLIM for derivation of structural and functional information was attempted [70]
Jerjies et al.	2010	Ex- vivo	SS-OCT successfully identified malignant changes in suspicious oral lesions ($n = 34$) through analysis of four variables [40]
Ahn et al.	2011	Hamster pouch	3D-OCT and polarimetry were combined, which helped in the identification of oral cancer field cancerization areas and lesion margins ($n = 9$) [69]
Hamdoon et al.	2012	Ex vivo	OCT capable to identify difference between normal and diseased oral mucosa through evaluation of five microanatomical structures ($n = 78$ suspected oral lesions) [41]
	2013	Ex vivo	Wide spectrum of oral pathologies were studied ($n = 125$ lesions), which included 43 microinvasive carcinoma; accuracy was 82%, and kappa for intraobserver agreement was 0.72 for "need for biopsy" [43]
Pande et al.	2014	Hamster pouch	Automated classification of optical coherence tomography images for diagnosis of oral cancer in hamster cheek pouch [33]
Choi et al.	2014	In vivo	Devoted three-dimensional vascular perfusion maps were reconstructed using novel vessel extraction algorithms [56]
Lee et al.	2015	Instrument design	Constructed a wide-field polarization-sensitive swept-source OCT for in vivo oral application [47]
Yoon et al.	2015	Instrument design	Constructed in vivo wide-field reflectance imaging and polarization-sensitive OCT to procure both morphological and fluorescence information [46]

(continued)

Table 11.1 (continued)

Author	Year	Study type	Findings
Hamdoon et al.	2016	In vivo	OCT assessment of surgical margins (n = 112 margins in 28 (T1-T2 N0 M0) OSCC cases). Positive margins showed elevated epithelial thickness [44]
Pande et al.	2016	Hamster pouch	Automated classification of fluorescence lifetime imaging (FLIM) and combined OCT data for diagnosis of oral cancer in hamster pouch, with comparatively high sensitivity and specificity [71]
Lee et al.	2016	In vivo	Biopsy guidance of oral lesions using wide-field OCT and automated segregation of images [55]
Tsai et al.	2017	In vivo	High-resolution images of oral mucosa microcirculation were obtained [57]. "Microcirculation" may evolve as a novel OCT signature with high potential for oral cancer detection
Wei et al.	2017	In vivo	Three-dimensional images of microcirculation and quantitative metrics of capillary loop density were possible [58]

dysplasia, to squamous cell carcinoma (SCC), on application of carcinogens such as 7,12-dimethylbenzanthracene (DMBA). The earliest reported studies are by Matheny et al. [30] and Wilder-Smith et al. [34] who carried out feasibility studies and demonstrated OCT-based malignancy detection in the HBP model. While Matheny et al. employed 22 animals, and carried out both in vivo and ex vivo studies, and obtained good resolution to a depth of 1–3 mm, Wilder-Smith et al., from the same laboratory, performed in vivo studies on 36 animals and imaged epithelial and subepithelial changes. Their findings suggested that epithelial and subepithelial structures could be clearly distinguished, and corresponding histopathological analysis of the tissues suggested 80% concordance. The same group carried out further studies using 3D OCT image constructs and compared these with the gold standard histopathological images—both conventional and 3D images. The extent and localization of tumor margins were visualized to confirm dysplastic and malignant changes [31]. HBP tissues were assessed using parallel frequency-domain optical coherence tomography (FDOCT) and a thermal light source by Graf et al. [38] who in another study also assessed nuclear morphology via spectral oscillations while investigating HBP precancerous lesions [32]. Pande et al. attempted to develop automated algorithms to quantify malignancy-specific structural features of the oral epithelium by processing OCT data from HBP tissues. Statistical classification model based on this algorithm yielded sensitivity and specificity of 90.2% and 76.3%, respectively [5]. In another study, OCT was carried out on carcinogen-treated and normal HBP tissues [24]. Tissues corresponding to early and late stages of carcinogen-induced carcinogenesis were investigated. OCT images showed well-distinguished layers of epithelial and subepithelial layers in most controls and early week DMBA-treated tissues. Two control tissues also showed disrupted epithelial architecture. These observations were also confirmed by Raman spectroscopy and was attributed to repeated injuries incurred by regular pulling out of buccal pouches [37]. Several multimodal applications of OCT in conjunction with other optical techniques have been employed in pursuit of better sensitivity and specificity to distinguish cancerous and healthy conditions. Such studies are described in the section on "Multimodal Applications."

11.3.2 Ex Vivo Studies

OCT of ex vivo cancerous and oral potentially malignant conditions has been explored and compared with histopathology in several studies. A report on ex vivo imaging of an oral cancer sample with an SS-OCT system (axial resolution: 8 μm) suggested distinction of abnormal regions

from normal regions [40]. In 2010, Jerjes et al. in a study on 34 oral lesions in 27 subjects, two clinicians blinded to histological diagnosis correctly segregated cases where biopsy was actually necessary; but the basement membrane was recognized only in 15 lesions [39]. Keratin cell layer identification and structural alterations in the layers have been shown in 87% of the cases in a cohort of 78 cancer subjects. Epithelial layer and basement membranes could be distinguished with an accuracy of 93.5% and 94%, respectively. An accuracy of 64% for blood vessels, 58% for salivary gland ducts, and 89% for rete pegs was also observed [41].

Ex vivo analysis of fibro-epithelial polyps, mild dysplasia, and moderate/severe dysplasia suggested epithelial differentiation as a function of depth and optical scattering from the cell nuclei. Mucosal layers in OCT images of oral dysplasia were not clear because of the higher density of abnormal cell nuclei, which impede light penetration. 3D-OCT datasets from same samples showed classification of biopsy samples into normal/mild and moderate/severe groups [42]. A major prospective study involving 125 suspicious lesions (125 subjects) utilized 2 independent team of readers to assess OCT images, which showed a sensitivity of 85%, specificity of 78%, and accuracy of 82%. Kappa coefficient of interobserver agreement was 0.72 on "the need for biopsy" [43]. Hamdoon et al. have also shown valuable application of OCT in the assessment of resection margins [44]. Their study on 112 margins (28 subjects) revealed 22 tumor-associated margins and 90 tumor-free margins. OCT accuracies for two independent expert readers were 88% and 84%, with an interobserver agreement as "very good" for superior, inferior, and medial margins and "good" for lateral surgical margin [44]. Birefringence can also be a potential parameter to distinguish healthy and cancerous tissues. A recent study involving eight oral mandibular tissues exploited in spectral domain polarization-sensitive optical coherence tomography (SD-PSOCT) suggested that monitoring of tissue birefringence along with backscattered intensity allows discrimination to differentiate between normal and cancerous lesions [45]. In relation to PSOCT, two previous studies had indicated that healthy buccal mucosa has higher birefringence compared to normal tongue tissue [46] and submucosal fibrosis has higher birefringence compared to adjoining normal mucosa [47]. PSOCT can pave way for distinguishing abnormal sites, based on collagen distribution.

11.3.3 In Vivo Clinical Studies

One of the earliest in vivo OCT studies imaged oral hard and soft tissues [48]. Several regions of the oral mucosa, including the masticatory mucosa (hard palate, gingival mucosa), the lining mucosa (soft palate, alveolar, buccal mucosa), the specialized mucosa (dorsum of the tongue), as well as the tooth structure, were imaged. The various types of keratinized and nonkeratinized mucosa could be distinguished with high accuracy [48]. Normal as well as abnormal gingiva and buccal mucosa classification was shown in 2005 [49]. In an attempt to explore further regions adjacent to oral mucosa, the mucosa of oropharynx was imaged ($n = 41$) during operative endoscopy. OCT imaging, in conjunction with endoscopic photography for gross and histologic image correlation, provided important microanatomical information for normal and pathological sites, with distinct zones of "normal, altered, and ablated tissue microstructures" for each pathology studied [50].

In order to discriminate successive cancer stages, several indicators may be needed to achieve good specificity. Swept-source OCT (SS-OCT) system data often uses three primary indicators—standard deviation (SD) and exponential decay constant (α) of an A-mode-scan spatial-frequency spectrum and the epithelium thickness—to distinguish normal and pathological tissues. Usually, in abnormal mucosa, the SD increases, α becomes smaller, and the epithelium becomes thicker. Studies have been carried out to evaluate the accuracy of these indicators. It is shown that SD and α are good diagnostic indicators for moderate dysplasia and squamous cell

carcinoma (SCC), while epithelial thickness can discriminate epithelia hyperplasia and moderate dysplasia [51]. The field of diagnostic OCT experienced a surge in the number of studies undertaken after these initial reports. Some of these studies include differentiating oral lesions at different stages of carcinogenesis [22], oral dysplasia and malignancy (n = 50) [21], labial gland imaging using handheld SS-OCT system for healthy volunteers (n = 5) in both two and three dimensions [52], and lesions of upper aerodigestive tract (n = 52, 100 lesions) [53].

As mentioned previously, information about various parameters/indicators representing normal/healthy tissues can be of great importance while analyzing abnormal tissues. Normal values of oral epithelial thickness can thus be one such reference value. This was attempted on a large sample size of 143 healthy subjects, and epithelial thickness was measured at seven different locations. Buccal mucosa (294 μm) and the hard palate (239 μm) showed highest thickness, whereas the floor of the mouth (99 μm) showed the thinnest epithelium [20].

While OCT is a potential tool for oral cancer diagnosis, better results can also be achieved by improvements in methods of image analysis. Many research groups have tried to achieve this through innovative approaches. A procedure for analyzing OCT images involved plotting of the boundary between the layers of epithelium (EP) and lamina propria (LP) to determine the EP thickness and estimate distribution of dysplastic cells, based on standard deviation (SD) mapping. Laterally average range of 70% SD in the EP was shown to be a reasonable threshold for differentiating moderately dysplastic lesions (n = 44) from mild dysplastic ones (n = 39), with sensitivity and specificity of 82% and 90%, respectively [54].

Like other optical techniques, the field of OCT is continually evolving, and advancements are being made by several groups to improve instrumentation, image acquisition, and processing. For better in vivo results, an imaging device must be able to access lesions located anywhere in the oral cavity and should have a sufficient field of view (FOV) to scan extensively wide like leukoplakia lesions. Lee et al. in 2015 reported a handheld OCT device with a large FOV that enabled rapid volumetric imaging in a single acquisition. The use of fast rotary pullback catheters (RPC) facilitated easy placement of probe on lesions. Thus, this system could scan suspicious lesion in most of the regions of oral cavity in a clinically implementable time. With this system, 176 in vivo OCT volumes (51 subjects) were scanned for a range of lesions from scars to dysplasia and SCC, as well as contralateral sites. Birefringence may always give additional insights which can be further explored [47]. Wide-field imaging has also been explored to address issues such as automated segmentation of images [55].

In the recent times, OCT has evolved as an angiography tool for evaluation of oral mucosa microcirculation [56–58]. In a report by Maslennikova et al. who followed radiation therapy patients, for oropharyngeal and nasopharyngeal carcinoma, a dose-dependent microvascular reaction to radiation injury was shown, even before the early clinical signs of mucositis [59]. Microcirculation can be a potential biomarker, as angiogenesis is an important feature of advanced oral cancers and may be used for evaluation of oral cancer recurrence in patients following radiotherapy/chemotherapy.

11.4 Quest for Improved Oral Cancer Diagnosis

A major limitation associated with OCT is morphologically and optically similar scattering properties of different pathological tissues; it is sometimes difficult to optically detect early-stage cancers simply on the basis of conventional OCT imaging [60, 61]. While several improvements in the conventional OCT mechanism are regularly reported, other approaches are also being explored for improved diagnosis. We have discussed two such approaches in this chapter. The first approach involves multimodal applications where OCT in combination with other optical techniques is exploited to yield comparatively improved results than when the techniques are used individually. Another approach involves contrast enhancement mechanisms coupled with OCT.

11.4.1 Multimodal Applications

Individual optical modalities are typically sensitive to a small aspect of abnormal and pathological changes. Two or more imaging modalities when combined can simultaneously probe several tissue characteristics to elucidate pathological changes and provide better sensitivity and specificity, compared to a single modality. Multimodal systems have combined OCT with several modalities, including multiphoton microscopy [62], fluorescence spectroscopy [63], fluorescence lifetime imaging (FLIM) [64], multiphoton tomography [65], and Raman spectroscopy (RS) [66, 67]. Out of these modalities, some of them have been explored in oral cancers as well. However, the disparate optical requirements, different optical sources, and wavelengths sometimes limit their widespread clinical applications. Moreover, such multimodal approaches would be more useful if the light sources and detection elements can be coupled in a single instrument which will also help achieve image registration and correlation.

OCT and Polarimetry: Both ex vivo and in vivo imaging, using HBP model ($n = 9$), to assess the efficacy of combined polarimetry [68] and OCT, have revealed information on epithelial and subepithelial changes during carcinogenesis [69]. The polarimetry technique identified up to five times increased retardance in sites with SCC and up to three times increased retardance in dysplastic sites, when compared with normal tissues.

FLIM and OCT: Co-registered OCT/FLIM images from multiple 2×2 mm^2 regions of HBP tissues have been shown. While the OCT images have shown thickening of epithelial layer, and loss of layered structure, the FLIM images suggested higher nicotinamide adenine dinucleotide and reduced collagen emission within the cancerous regions [64, 70]. A recent study combining FLIM and OCT obtained an accuracy of 87.4%, better than accuracy based on only FLIM (83.2%) or OCT (81.0%). The complementary information provided by combined FLIM-OCT features showed high sensitivity and specificity for discriminating benign (88.2% and 92.0%), precancerous (81.5% and 96.0%), and cancerous (90.1% and 92.0%) stages [71].

RS and OCT: RS-OCT images compensate for limitations of both the techniques. Microstructural and biochemical features of dental caries analyzed using RS and OCT were reported in 2005 [66]. Dual-modal device capable of sequential RS-OCT image acquisition along a common optical axis that could utilize NIR to acquire data through common sampling optics [67] and integrated common clinical probe [72] is reported. Cancerous and normal HBP tissues probed by both OCT and RS have been investigated [24]. In a combined Raman and OCT study on HBP tissues, OCT images have shown well-distinguished layers of epithelial and subepithelial layers in most controls and early week DMBA-treated tissues; however, some control tissues corresponding to higher duration of carcinogen application showed disrupted epithelial architecture. Representative OCT images of HBP tissues, healthy and carcinogen treated for 9 and 13 weeks, are shown in Fig. 11.3. These observa-

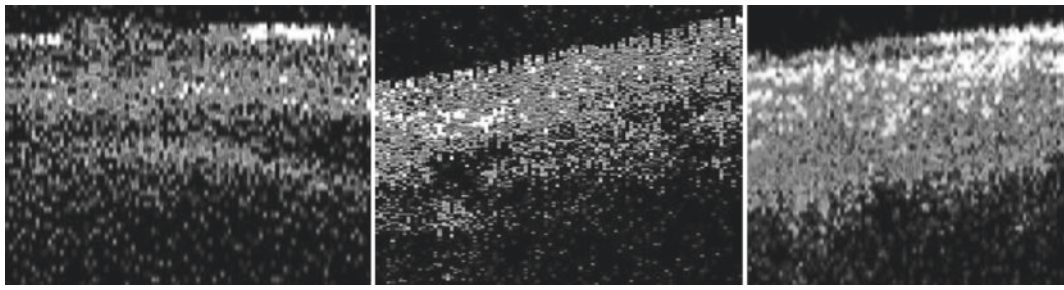

Fig. 11.3 OCT images of healthy control showing layered structures, and DMBA-treated tissues after 9 and 13 weeks showing disrupted architecture of epithelium. Week 13 tissues showing complete disruption of epithelium

tions, also confirmed by RS, were attributed to repeated injuries incurred during regular pulling out of buccal pouches for carcinogen application and regular observations [37]. Thus, combined application of RS and OCT provided an unbiased confirmation of the findings.

RCM and OCT: Reflectance confocal microscopy (RCM) is another emerging noninvasive imaging technique that enables an en face tissue visualization at the cellular level with good lateral and axial dimensions [46, 73]. Multimodal endoscopic systems that combine wide-field reflectance and fluorescence imaging with PS-OCT have been explored for human oral cavity. Wide-field reflectance/fluorescence imaging provided information of tissue surface based on reflectance and fluorescence, while PS-OCT provided information about subsurface structures and birefringence. Wide-field imaging with adjustable depth of focus (DOF) was used for high-sensitivity guided imaging [46].

RCM systems usually adapt optics with high focusing power for high lateral resolution, but the axial resolution is typically more than three times worse than the lateral resolution [73] due to anisotropic light propagation.

A full-field optical coherence tomography (FF-OCT) system can be considered as a light microscope with the axial resolution assisted by the coherence gating effect of OCT (Fig. 11.4). Compared to SD-OCT used in ophthalmic application, FF-OCT is a TD-OCT technique using a camera as detector to increase the scanning speed of traditional TD-OCT system (Fig. 11.5). A FF-OCT images all the lateral pixels simultaneously and performs axial scanning and dynamic focusing at the same time. By using high focusing power optics, lateral resolution similar to RCM can be achieved; accompanied with a broadband light source and corresponding narrow coherent gate, a FF-OCT system can achieve cellular resolution in all three dimensions (Fig. 11.4). FF-OCT can provide 3D in vivo image of oral tissue with 1 μm resolution and several hundred microns penetration depth. In the cross-sectional view of FF-OCT image, the boundary of epithelial and lamina propria layer can be distinguished which is an important information for oral cancer detection in the early stage. For reference purpose we have obtained in vivo OCT images in a healthy volunteer to show the lip, tongue, and skin microanatomy and tissue architecture at different depths, at nearly cellular resolution (refer to Figs. 11.6, 11.7, and 11.8). In the stratified squamous epithelial layer, the squamous cells are more keratinized with thinner thickness and irregular shape which can be observed in the OCT cross-sectional and en face images. The taste buds of tongue mucosa can be detected between the boundary of epithelial and lamina propria layer (Fig. 11.7). In the lamina propria layer, the features of elastic and collagen fiber which are parallel to the epithelium can be observed in the OCT cross-sectional image. The FF-OCT images correspond well with histology as RCM does, but the thickness of cell and tissue layer can be better distinguished with cross-sectional view of OCT images.

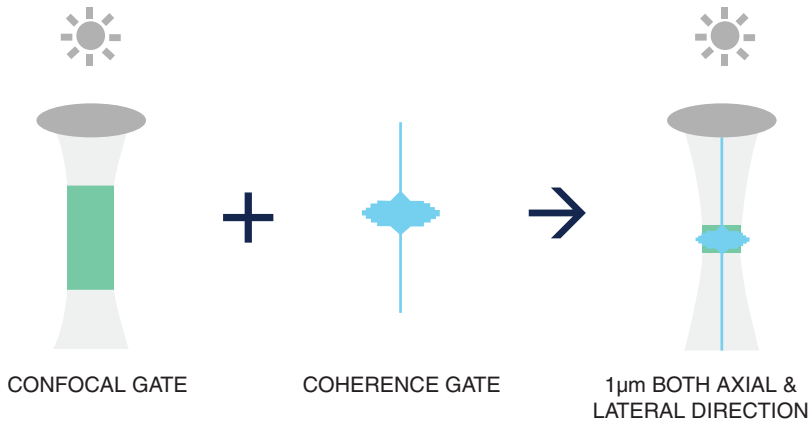

Fig. 11.4 Through confocal and coherence gating, excellent axial and lateral resolution can be achieved

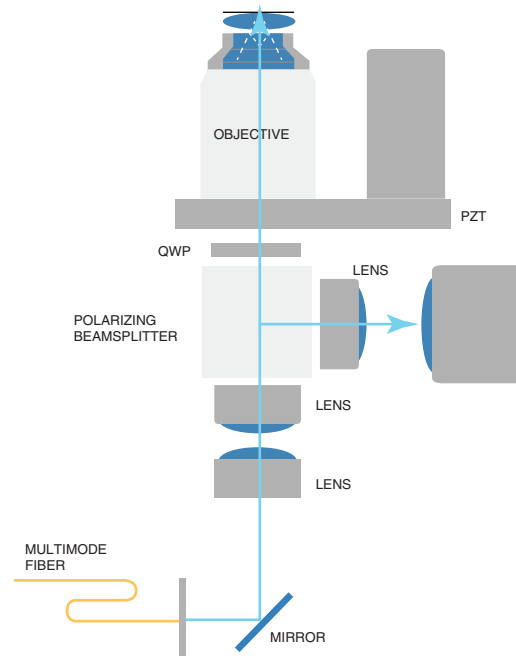

Fig. 11.5 Dissection of (Mirau-based) full-field OCT imaging system (PZT, piezoelectric transducer; QWP, quarter wave plate)

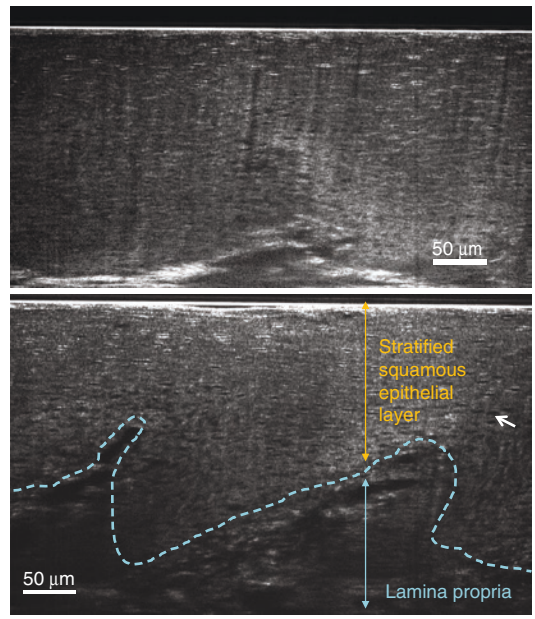

Fig. 11.6 The 3D cross section of in vivo OCT images (natural logarithmic gray level, 32 bit filtered by ImageJ) is of the lip taken in a healthy volunteer (41-year-old male). The dotted blue line indicates the epidermis-dermis junction, and the orange line indicates the thickness of the stratified squamous epithelium. The white arrow (showing the dark hole) indicates the nucleus of stratum spinosum. The incident power unto the sample and CCD exposure time are 4.5 mW and 2.7 milliseconds. The 3D cross-sectional images at different depths, 7 µm (panel **a**), 38 µm (panel **b**), 105 µm (panel **c**), 203 µm (panel **d**), 292 µm (panel **e**), are shown along with the oblique sections (panel **f**)

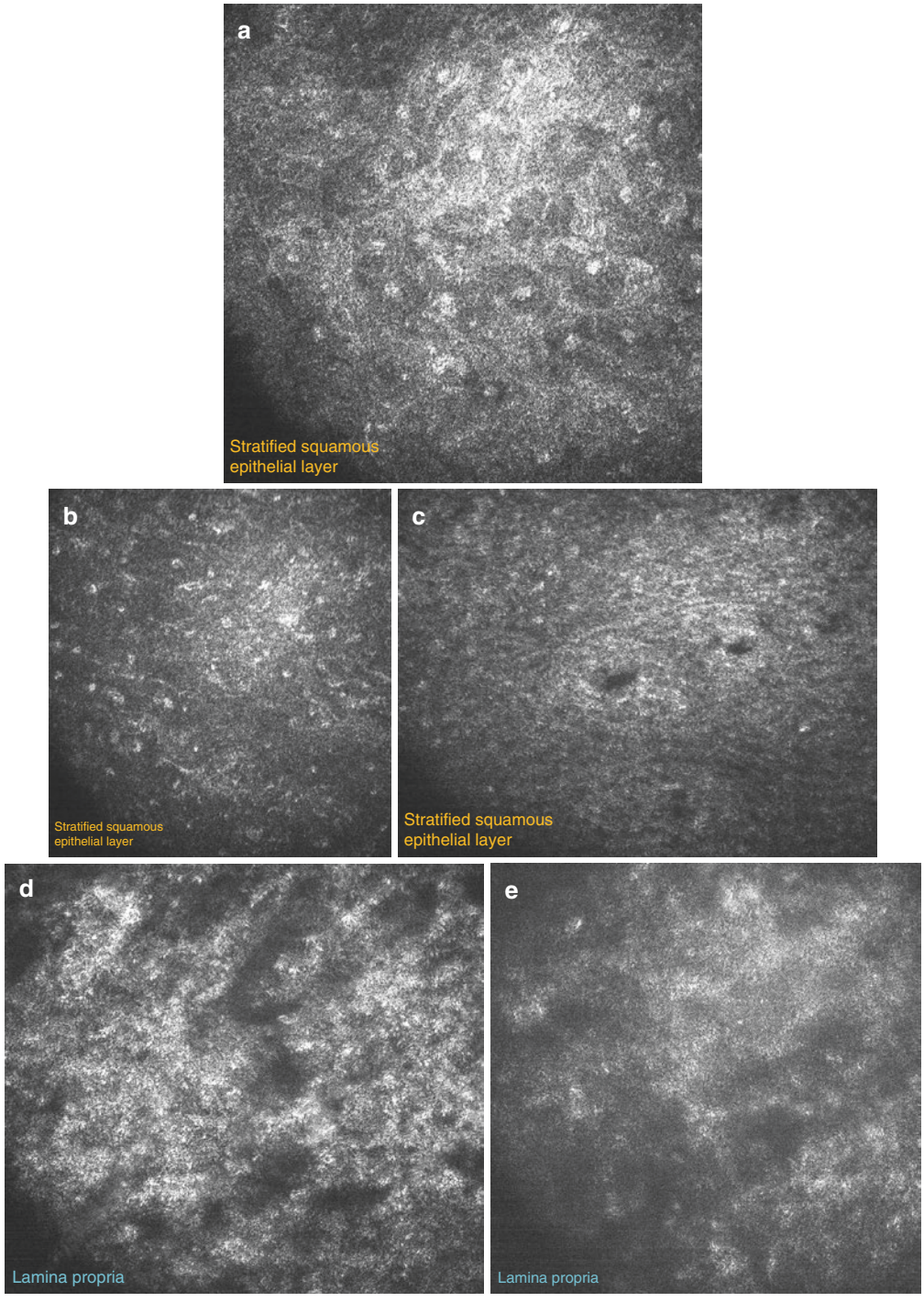

Fig. 11.6 (continued)

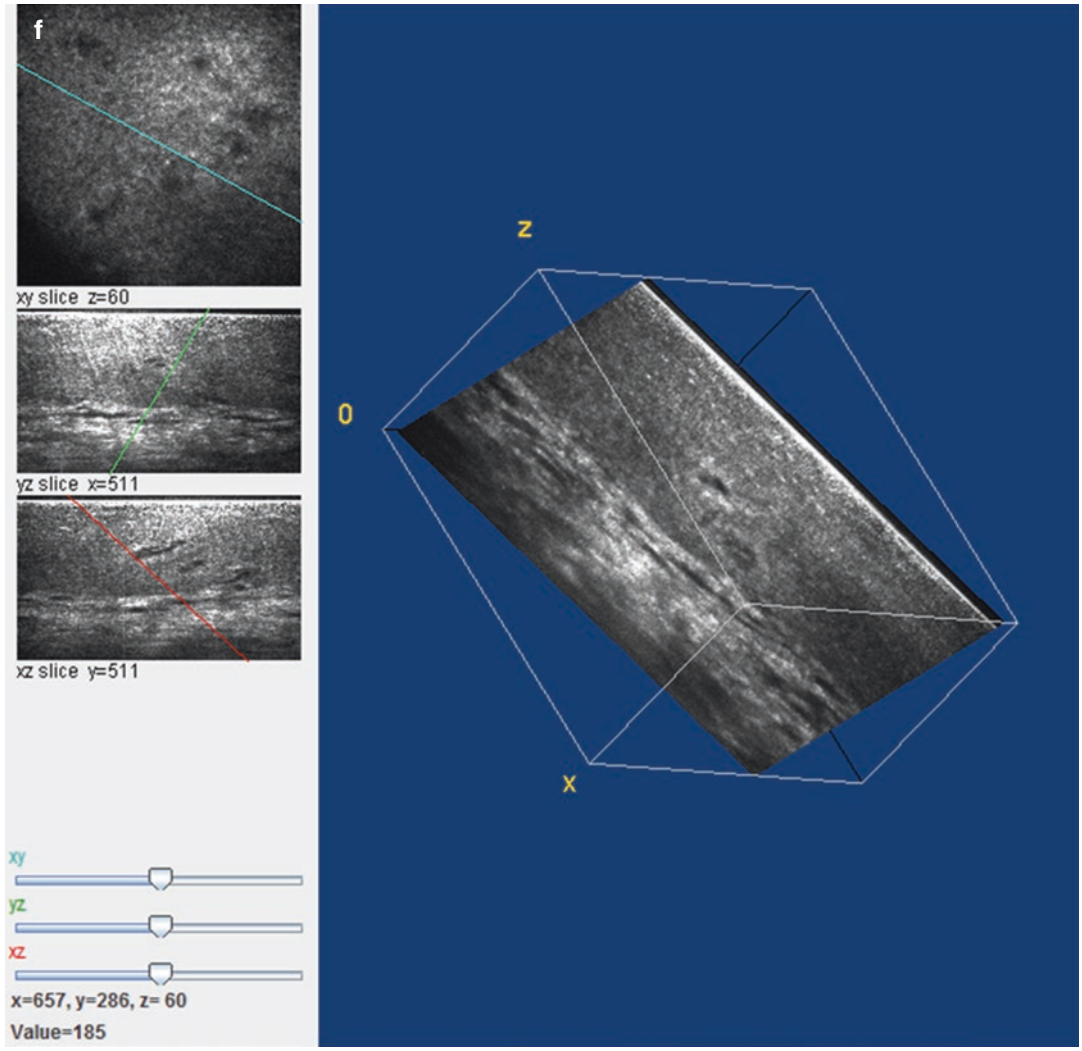

Fig. 11.6 (continued)

In view of complexity of biological phenomena, a single technique may not be sufficient to probe tissue characteristics, especially in case of cancers. Multimodal optical techniques can thus provide additional and complementary information from the same tissue and helps in better understanding of the biological complexity. A simple example can be of scars that leads to thickening due to fibrosis and alteration in the layered structure. OCT images alone can misinterpret them as cancerous, whereas fluorescence spectroscopy would suggest presence of collagen (healthy), rather than changes in NADH/FAD (indicator of possible cancerous changes). Multimodal application can thus be instrumental in preventing misdiagnosis.

11.4.2 Contrast Improvement

Although there is more progress in developing contrast agents to enhance OCT images in vivo, several contrast agents [74, 75] have been explored to overcome limitations. Contrast-

enhancing mechanisms coupled with OCT will be useful. Spectroscopic OCT (SOCT) [76], pump and probe techniques [77], engineered microspheres [61], microbubbles [75], and nanocages or nanoparticles [78] are some of the reported methods.

SOCT utilizes the relative spectral difference between source and backscattered signals to measure absorption and scattering. However, SCOT can identify only those features with absorption scattering less than the source bandwidth. OCT contrast enhancement can also be achieved by exploiting nonlinear processes such as coherent anti-Stokes Raman scattering (CARS) and second harmonic generation. Research group led by Prof. Stephen Boppart has been working in this field using broadband illumination for imaging purposes, as well as molecular level contrast enhancement [60]. Pump and probe-based contrast enhancement for OCT imaging relies on transient absorptions in a sample that can be induced by an external pump

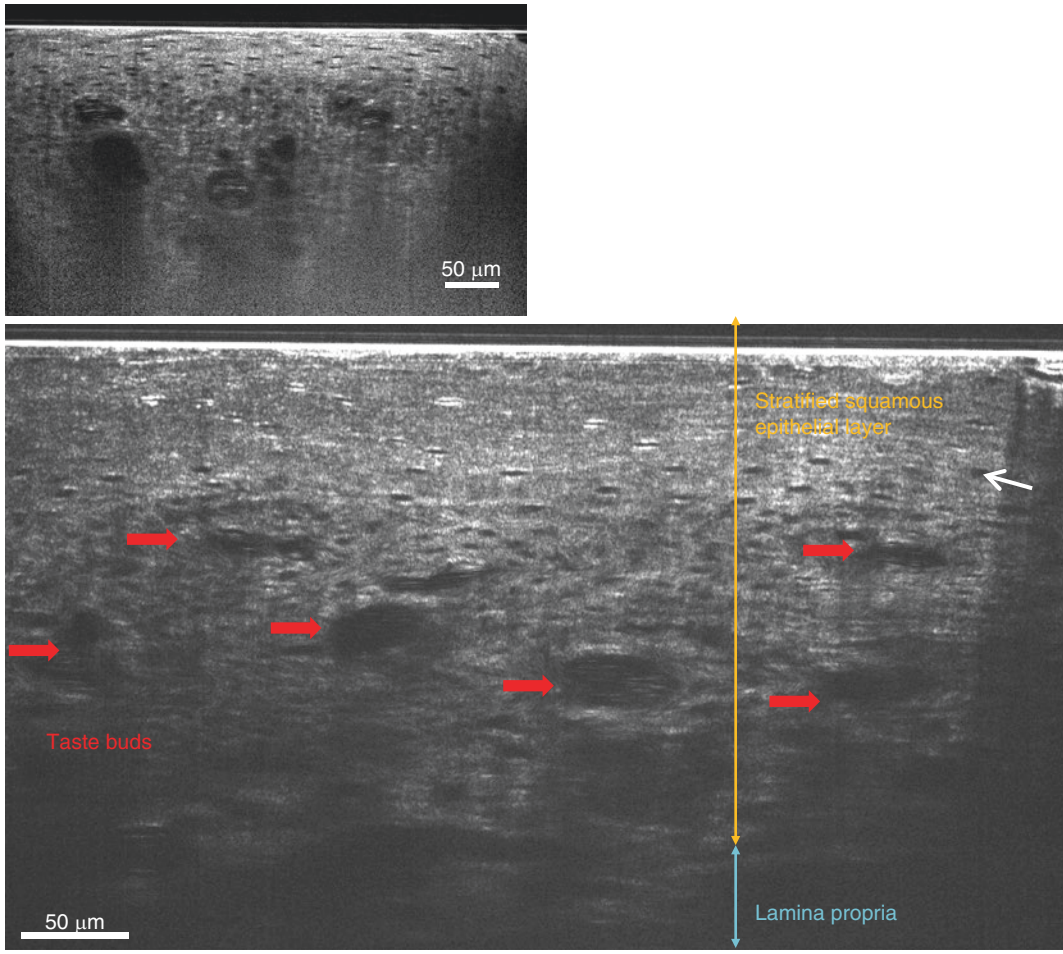

Fig. 11.7 The 3D cross section of in vivo OCT images are (natural logarithmic gray level, 32 bit depth filtered by ImageJ) of oral tongue taken in a healthy volunteer (41-year-old male). The dotted blue line indicates the epidermis-dermis junction, and the orange line indicates the thickness of the stratified squamous epithelium, and the red arrows are pointing the taste buds. The white arrow (showing the dark hole) indicates the nucleus of stratum spinosum. The incident power unto the sample and CCD exposure time are 4.5 mW and 2.7 ms. The cross-sectional images are shown at different depths: 40 μm (panel **a**), 64 μm (panel **b**), 113 μm (panel **c**), 181 μm (panel **d**) which are shown along with the oblique sections (panel **e**)

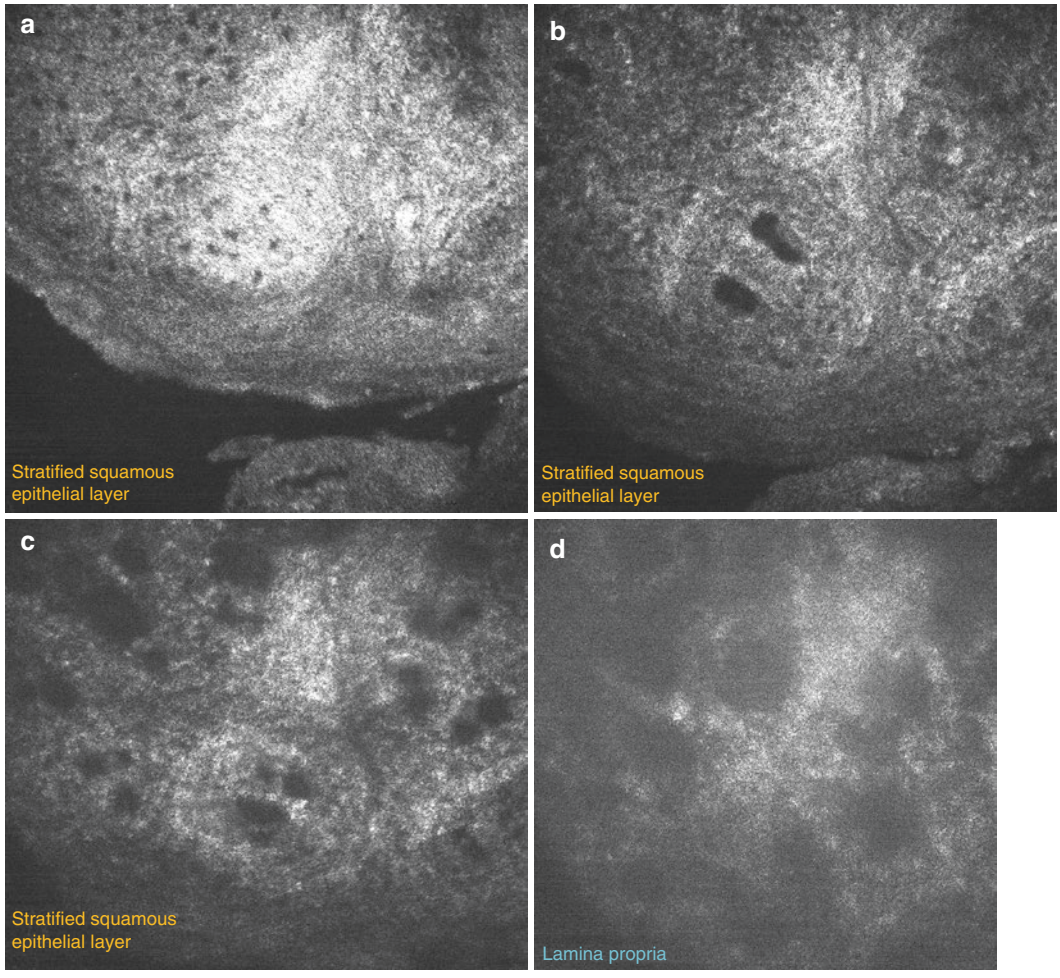

Fig. 11.7 (continued)

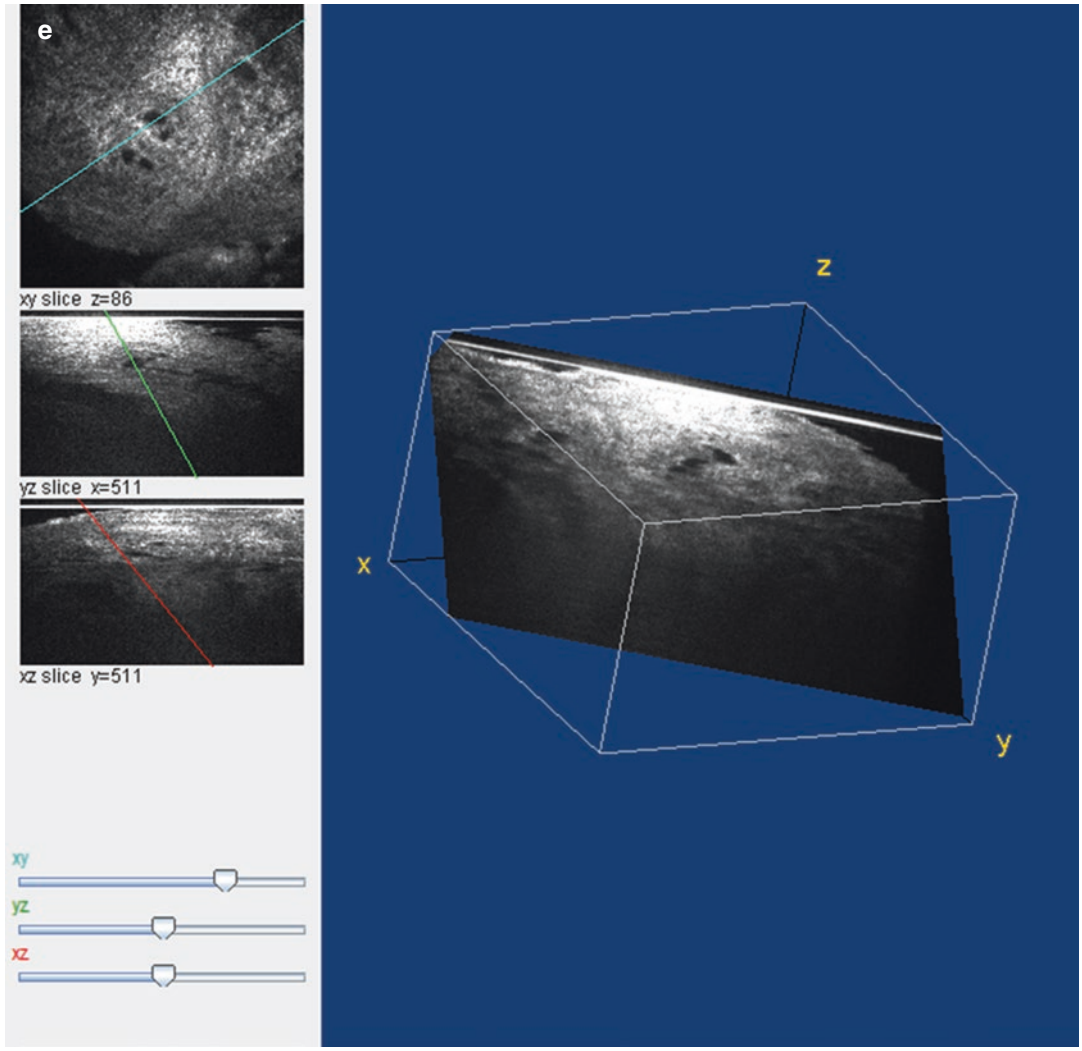

Fig. 11.7 (continued)

beam. However, this method requires introduction of different contrast agents, depending on the excitation source and the transient spectra of the molecules being investigated [76]. An alternative contrast enhancement method is using exogenous contrast agents like engineered microspheres that can change the absorption and scattering properties. These microspheres change the absorption and scattering characteristics in selected regions and can be targeted to structures like cellular receptors [61]. Most of these methods that are currently being used for contrast enhancement need a contrast agent. Moreover, further biomedical explorations are required to assess their success. Therefore, more studies and new techniques could help eliminate this limitation.

Nanoparticles (NPs), such as nanospheres, nanocages, nanoshells, and nanorods, have been explored to overcome OCT limitations by enhancing the contrast [78–80] but with limited in vivo success till date. Gold nanoparticles (Au NPs) are promising contrast agents as they are biocompatible, easy to synthesize, and can be specifically targeted through functional moieties. Moreover, optical resonance properties of Au

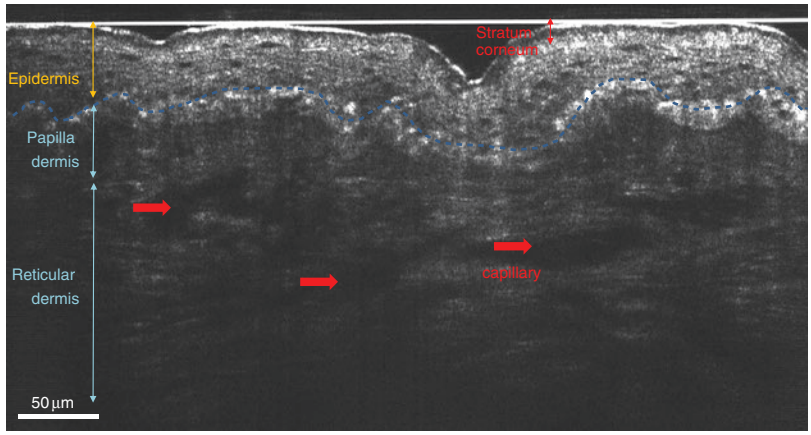

Fig. 11.8 In vivo OCT image of the skin from a healthy volunteer (age 41-year-old male). The dotted blue line indicates the epidermis-dermis junction, and the orange line indicates the thickness of the epidermis. The blue lines indicate the thicknesses of the papilla and reticular dermis. The red line indicates the thickness of the stratum corneum. Melanin can be observed on the epidermis-dermis junction which show white spot feature. The keratinocytes can be observed in the epidermis layer. In the dermis layer, the patterns of papilla and reticular dermis can be distinguished, and capillary can be seen in this layer too. The incident power unto the sample and CCD exposure time are 4.5 mW and 2.7 ms

NPs can be controlled by modifying their shapes and sizes [81]. One potential method is the topical application of gold nanoparticles on the epithelial surface. Moreover, topical application as compared to systemic administration can reduce toxicity burden, often associated with metallic nanoparticles. The stratum corneum, which is the uppermost layer of the oral epithelium is thick and can act as a biological barrier to the delivery of NPs. Kim et al. overcame this barrier in HBP model using microneedles assisted by ultrasound forces [82]. Recently developments have shown encouraging results with severalfold enhancements and increased depth of penetration. These studies have shown picomolar level sensitivity useful in in vivo imaging [83]. This approach still suffers from potential limitations including toxicity and poor in vivo delivery and distribution.

Conclusion

OCT can be used to obtain functional optical biopsies. OCT imaging combined with quantification of physiological functional parameters such as perfusion/oxygenation and cellular organization and improvements in signal analysis can allow achievement of goal. For better in vivo results, an imaging device must be able to access lesions located anywhere in the oral cavity where lesions may be actually located and should have a sufficient field of view (FOV) to quickly scan extensive lesions in a clinically feasible timing. Recent advancements in the field of OCT-based biomedical diagnosis suggest OCT can be an effective tool in oral cancer diagnosis. Limitations in OCT images can be overcome through multimodal application with other optical techniques like white-light fluorescence and photo-acoustic imaging as well as through contrast improvement. Availability of handheld OCT probe can serve as a real-time chairside diagnostic tool. Though it is extremely difficult to reach the accuracy of conventional histopathology, with the rapid advancement in biomedical engineering and computation, in the nearest future OCT can become a useful adjunct to chairside clinical examination, to screen suspected oral lesions, particularly to rule out oral cancers. Overall, OCT has a strong potential to be a noninvasive imaging technique and clinically useful diagnostic adjunct.

Acknowledgment We thank Yunglin David Ma and Allen Lin from Apollo Medical Optics, Ltd. for their cooperation.

References

1. Huang D, Swanson E, Lin C, Schuman J, Stinson W, Chang W, Hee M, Flotte T, Gregory K, Puliafito CA, et al. Optical coherence tomography. Science. 1991;254:1178–81.
2. Fujimoto JG. Optical coherence tomography for ultrahigh resolution *in vivo* imaging. Nat Biotechnol. 2003;21:1361–7.
3. Drexler W, Morgner U, Ghanta RK, Kärtner FX, Schuman JS, Fujimoto JG. Ultrahigh-resolution ophthalmic optical coherence tomography. Nat Med. 2001;7:502–7.
4. An L, Wang RK. In vivo volumetric imaging of vascular perfusion within human retina and choroids with optical micro-angiography. Opt Express. 2008;16:11438–52.
5. Boppart SA, Luo W, Marks DL, Singletary KW. Optical coherence tomography: feasibility for basic research and image-guided surgery of breast cancer. Breast Cancer Res Treat. 2004;84:85–97.
6. Vakoc BJ, Fukumura D, Jain RK, Bouma BE. Cancer imaging by optical coherence tomography: preclinical progress and clinical potential. Nat Rev Cancer. 2012;12:363–8.
7. Wessels R, De Bruin D, Faber D, Van Leeuwen T, Van Beurden M, Ruers T. Optical biopsy of epithelial cancers by optical coherence tomography (OCT). Lasers Med Sci. 2014;29:1297–305.
8. Bezerra HG, Costa MA, Guagliumi G, Rollins AM, Simon DI. Intracoronary optical coherence tomography: a comprehensive review: clinical and research applications. J Am Coll Cardiol Intv. 2009;2:1035–46.
9. Larina IV, Ivers S, Syed S, Dickinson ME, Larin KV. Hemodynamic measurements from individual blood cells in early mammalian embryos with Doppler swept source OCT. Opt Lett. 2009;34:986–8.
10. Olmedo JM, Warschaw KE, Schmitt JM, Swanson DL. Optical coherence tomography for the characterization of basal cell carcinoma in vivo: a pilot study. J Am Acad Dermatol. 2006;55:408–12.
11. Mogensen M, Joergensen TM, Nürnberg BM, Morsy HA, Thomsen JB, Thrane L et al. Assessment of optical coherence tomography imaging in the diagnosis of non-melanoma skin cancer and benign lesions versus normal skin: observer-blinded evaluation by dermatologists and pathologists. Dermatol Surg. 2009;35:965-72.
12. Jørgensen TM, Tycho A, Mogensen M, Bjerring P, Jemec GB. Machine-learning classification of non-melanoma skin cancers from image features obtained by optical coherence tomography. Skin Res Technol. 2008;14:364–9.
13. Wong BJ, Jackson RP, Guo S, Ridgway JM, Mahmood U, Su J, Shibuya TY, Crumley RL, Gu M, Armstrong WB. In vivo optical coherence tomography of the human larynx: normative and benign pathology in 82 patients. Laryngoscope. 2005;115:1904–11.
14. Çilesiz I, Fockens P, Kerindongo R, Faber D, Tytgat G, ten Kate F, van Leeuwen T. Comparative optical coherence tomography imaging of human esophagus: how accurate is localization of the muscularis mucosae? Gastrointest Endosc. 2002;56:852–7.
15. Cobb MJ, Hwang JH, Upton MP, Chen Y, Oelschlager BK, Wood DE, Kimmey MB, Li X. Imaging of subsquamous Barrett's epithelium with ultrahigh-resolution optical coherence tomography: a histologic correlation study. Gastrointest Endosc. 2010;71:223–30.
16. Pitris C, Jesser C, Boppart SA, Stamper D, Brezinski ME, Fujimoto JG. Feasibility of optical coherence tomography for high-resolution imaging of human gastrointestinal tract malignancies. J Gastroenterol. 2000;35:87–92.
17. Poneros JM, Brand S, Bouma BE, Tearney GJ, Compton CC, Nishioka NS. Diagnosis of specialized intestinal metaplasia by optical coherence tomography. Gastroenterology. 2001;120:7–12.
18. Escobar P, Belinson J, White A, Shakhova N, Feldchtein F, Kareta M, et al. Diagnostic efficacy of optical coherence tomography in the management of preinvasive and invasive cancer of uterine cervix and vulva. Int J Gynecol Cancer. 2004;14:470–4.
19. Tearney G, Brezinski M, Southern J, Bouma B, Boppart S, Fujimoto J. Optical biopsy in human urologic tissue using optical coherence tomography. J Urol. 1997;157:1915–9.
20. Prestin S, Rothschild SI, Betz CS, Kraft M. Measurement of epithelial thickness within the oral cavity using optical coherence tomography. Head Neck. 2012;34:1777–81.
21. Wilder-Smith P, Lee K, Guo S, Zhang J, Osann K, Chen Z, Messadi D. In vivo diagnosis of oral dysplasia and malignancy using optical coherence tomography: preliminary studies in 50 patients. Lasers Surg Med. 2009;41:353–7.
22. Tsai M-T, Lee C-K, Lee H-C, Chen H-M, Chiang C-P, Wang Y-M, Yang C-C. Differentiating oral lesions in different carcinogenesis stages with optical coherence tomography. J Biomed Opt. 2009;14:044027–8.
23. Ferlay J, Soerjomataram I, Dikshit R, Eser S, Mathers C, Rebelo M, Parkin DM, Forman D, Bray F. Cancer incidence and mortality worldwide: sources, methods and major patterns in GLOBOCAN 2012. Int J Cancer. 2015;136:E359–86.
24. Kumar P, Krishna CM, Sahoo NK, Rao KD. Multimodal spectroscopic applications in cancer diagnosis: combined Raman spectroscopy and optical coherence tomography. Asian J Phys. 2015;7
25. Takada K, Yokohama I, Chida K, Noda J. New measurement system for fault location in optical waveguide devices based on an interferometric technique. Appl Opt. 1987;26:1603–6.

26. Fujimoto JG, Pitris C, Boppart SA, Brezinski ME. Optical coherence tomography: an emerging technology for biomedical imaging and optical biopsy. Neoplasia. 2000;2:9–25.
27. Zysk AM, Nguyen FT, Oldenburg AL, Marks DL, Boppart SA. Optical coherence tomography: a review of clinical development from bench to bedside. J Biomed Opt. 2007;12:051403–21.
28. Wang Y, Zhao Y, Nelson J, Chen Z, Windeler RS. Ultrahigh-resolution optical coherence tomography by broadband continuum generation from a photonic crystal fiber. Opt Lett. 2003;28:182–4.
29. De Boer JF, Milner TE. Review of polarization sensitive optical coherence tomography and stokes vector determination. J Biomed Opt. 2002;7:359–71.
30. Matheny ES, Hanna NM, Jung WG, Chen Z, Wilder-Smith P, Mina-Araghi R, Brenner M. Optical coherence tomography of malignancy in hamster cheek pouches. J Biomed Opt. 2004;9:978–81.
31. Hanna NM, Waite W, Taylor K, Jung WG, Mukai D, Matheny E, et al. Feasibility of three-dimensional optical coherence tomography and optical Doppler tomography of malignancy in hamster cheek pouches. Photomed Laser Surg. 2006;24:402–9.
32. Graf RN, Robles FE, Chen X, Wax A. Detecting precancerous lesions in the hamster cheek pouch using spectroscopic white-light optical coherence tomography to assess nuclear morphology via spectral oscillations. J Biomed Opt. 2009;14:064030–8.
33. Pande P, Shrestha S, Park J, Serafino MJ, Gimenez-Conti I, Brandon J, Cheng Y-S, Applegate BE, Jo JA. Automated classification of optical coherence tomography images for the diagnosis of oral malignancy in the hamster cheek pouch. J Biomed Opt. 2014;19:086022.
34. Wilder-Smith P, Jung W-G, Brenner M, Osann K, Beydoun H, Messadi D, Chen Z. In vivo optical coherence tomography for the diagnosis of oral malignancy. Lasers Surg Med. 2004;35:269–75.
35. Jung W, Zhang J, Chung J, Wilder-Smith P, Brenner M, Nelson JS, Chen Z. Advances in oral cancer detection using optical coherence tomography. IEEE J Sel Top Quantum Electron. 2005;11:811–7.
36. Kumar P, Bhattacharjee T, Ingle A, Maru G, Krishna CM. Raman spectroscopy of experimental oral carcinogenesis: study on sequential cancer progression in hamster buccal pouch model. Technol Cancer Res Treat. 2016;15:NP60–72.
37. Kumar P, Bhattacharjee T, Pandey M, Hole AR, Ingle A, Murali Krishna C. Raman spectroscopy in experimental oral carcinogenesis: investigation of abnormal changes in control tissues. J Raman Spectrosc. 2016;47:1318.
38. Graf R, Brown W, Wax A. Parallel frequency-domain optical coherence tomography scatter-mode imaging of the hamster cheek pouch using a thermal light source. Opt Lett. 2008;33:1285–7.
39. Tsai MT, Lee HC, Lu CW, Wang YM, Lee CK, Yang CC et al. Delineation of an oral cancer lesion with swept-source optical coherence tomography. J Biomed Opt. 2008;13:044012.
40. Jerjes W, Upile T, Conn B, Hamdoon Z, Betz CS, McKenzie G, Radhi H, et al. In vitro examination of suspicious oral lesions using optical coherence tomography. Br J Oral Maxillofac Surg. 2010;48:18–25.
41. Hamdoon Z, Jerjes W, Al-Delayme R, McKenzie G, Jay A, Hopper C. Structural validation of oral mucosal tissue using optical coherence tomography. Head Neck Oncol. 2012;4:29.
42. Adegun OK, Tomlins PH, Hagi-Pavli E, Mckenzie G, Piper K, Bader DL, et al. Quantitative analysis of optical coherence tomography and histopathology images of normal and dysplastic oral mucosal tissues. Lasers Med Sci. 2012;27:795–804.
43. Hamdoon Z, Jerjes W, Upile T, McKenzie G, Jay A, Hopper C. Optical coherence tomography in the assessment of suspicious oral lesions: an immediate ex vivo study. Photodiagn Photodyn Ther. 2013;10:17–27.
44. Hamdoon Z, Jerjes W, McKenzie G, Jay A, Hopper C. Optical coherence tomography in the assessment of oral squamous cell carcinoma resection margins. Photodiagn Photodyn Ther. 2016;13:211–7.
45. Sharma P, Verma Y, Sahu K, Kumar S, Varma AV, Kumawat J, et al. Human ex-vivo oral tissue imaging using spectral domain polarization sensitive optical coherence tomography. Lasers Med Sci. 2017;32:143–50.
46. Yoon Y, Jang WH, Xiao P, Kim B, Wang T, Li Q, et al. In vivo wide-field reflectance/fluorescence imaging and polarization-sensitive optical coherence tomography of human oral cavity with a forward-viewing probe. Biomed Opt Express. 2015;6:524–35.
47. Lee AMD, Cahill L, Liu K, MacAulay C, Poh C, Lane P. Wide-field in vivo oral OCT imaging. Biomed Opt Express. 2015;6:2664–74.
48. Feldchtein FI, Gelikonov GV, Gelikonov VM, Iksanov RR, Kuranov RV, Sergeev AM, Gladkova ND, Ourutina MN, Warren JA, Reitze DH. In vivo OCT imaging of hard and soft tissue of the oral cavity. Opt Express. 1998;3:239–50.
49. C. Shu-Fan, L. Chih-Wei, T. Meng-Tsan, W. Yih-Ming, C.C. Yang, C. Chun-Ping, Oral Cancer Diagnosis with Optical Coherence Tomography, 2005 IEEE Engineering in Medicine and Biology 27th Annual Conference, 2005, pp. 7227–7229.
50. Ridgway JM, Armstrong WB, Guo S, et al. In vivo optical coherence tomography of the human oral cavity and oropharynx. Arch Otolaryngol Head Neck Surg. 2006;132:1074–81.
51. Tsai M-T, Lee H-C, Lee C-K, Yu C-H, Chen H-M, Chiang C-P, Chang C-C, Wang Y-M, Yang CC. Effective indicators for diagnosis of oral cancer using optical coherence tomography. Opt Express. 2008;16:15847–62.
52. Ozawa N, Sumi Y, Shimozato K, Chong C, Kurabayashi T. *In vivo* imaging of human labial glands using advanced optical coherence tomography.

Oral Surg Oral Med Oral Pathol Oral Radio Endod. 2009;108:425–9.
53. Volgger V, Stepp H, Ihrler S, Kraft M, Leunig A, Patel PM, Susarla M, Jackson K, Betz CS. Evaluation of optical coherence tomography to discriminate lesions of the upper aerodigestive tract. Head Neck. 2013;35:1558–66.
54. Lee CK, Chi TT, Wu CT, Tsai MT, Chiang CP, Yang CC. Diagnosis of oral precancer with optical coherence tomography. Biomed Opt Express. 2012;3:1632–46.
55. A.M. Lee, R. Goldan, H. Pahlevaninezhad, G. Hohert, K. Liu, C.E. MacAulay, et al, Towards biopsy guidance of oral lesions with wide-field OCT imaging, Biomedical Optics 2016, Optical Society of America, Fort Lauderdale, Florida, 2016, pp. JM4A4.
56. Choi WJ, Wang RK. *In vivo* imaging of functional microvasculature within tissue beds of oral and nasal cavities by swept-source optical coherence tomography with a forward/side-viewing probe. Biomed Opt Express. 2014;5:2620–34.
57. Tsai MT, Chen Y, Lee CY, Huang BH, Trung NH, Lee YJ, et al. Noninvasive structural and microvascular anatomy of oral mucosae using handheld optical coherence tomography. Biomed Opt Express. 2017;8:5001–12.
58. Wei W, Choi WJ, Wang RK. Microvascular imaging and monitoring of human oral cavity lesions in vivo by swept-source OCT-based angiography. Lasers Med Sci. 2018;33:123–34.
59. Maslennikova AV, Sirotkina MA, Moiseev AA, Finagina ES, Ksenofontov SY, Gelikonov GV, et al. In-vivo longitudinal imaging of microvascular changes in irradiated oral mucosa of radiotherapy cancer patients using optical coherence tomography. Sci Rep. 2017;7:16505.
60. Vinegoni C, Bredfeldt JS, Marks DL, Boppart SA. Nonlinear optical contrast enhancement for optical coherence tomography. Opt Express. 2004;12:331–41.
61. Lee TM, Oldenburg AL, Sitafalwalla S, Marks DL, Luo W, Toublan FJ-J, et al. Engineered microsphere contrast agents for optical coherence tomography. Opt Lett. 2003;28:1546–8.
62. Vinegoni C, Ralston T, Tan W, Luo W, Marks DL, Boppart SA, et al. Integrated structural and functional optical imaging combining spectral-domain optical coherence and multiphoton microscopy. Appl Phys Lett. 2006;88:053901.
63. Barton JK, Guzman F, Tumlinson A. Dual modality instrument for simultaneous optical coherence tomography imaging and fluorescence spectroscopy. J Biomed Opt. 2004;9:618–23.
64. Jo JA, Applegate BE, Park J, Shrestha S, Pande P, Gimenez-Conti IB, Brandon JL. *In Vivo* simultaneous morphological and biochemical optical imaging of oral epithelial Cancer. IEEE Trans Biomed Eng. 2010;57:2596–9.
65. König K, Speicher M, Bückle R, Reckfort J, McKenzie G, Welzel J, et al. Clinical optical coherence tomography combined with multiphoton tomography of patients with skin diseases. J Biophotonics. 2009;2:389–97.
66. Ko AC, Choo-Smith LP, Hewko M, Leonardi L, Sowa MG, Dong CC et al. Ex vivo detection and characterization of early dental caries by optical coherence tomography and Raman spectroscopy. J Biomed Opt. 2005;10:031118.
67. Patil CA, Bosschaart N, Keller MD, van Leeuwen TG, Mahadevan-Jansen A. Combined Raman spectroscopy and optical coherence tomography device for tissue characterization. Opt Lett. 2008;33:1135–7.
68. Bickel WS, Davidson J, Huffman D, Kilkson R. Application of polarization effects in light scattering: a new biophysical tool. Proc Natl Acad Sci USA. 1976;73:486–90.
69. Ahn Y-C, Chung J, Wilder-Smith P, Chen Z. Multimodality approach to optical early detection and mapping of oral neoplasia. J Biomed Opt. 2011;16:076007.
70. Park J, Jo JA, Shrestha S, Pande P, Wan Q, Applegate BE. A dual-modality optical coherence tomography and fluorescence lifetime imaging microscopy system for simultaneous morphological and biochemical tissue characterization. Biomed Opt Express. 2010;1:186–200.
71. Pande P, Shrestha S, Park J, Gimenez-Conti I, Brandon J, Applegate BE, et al. Automated analysis of multimodal fluorescence lifetime imaging and optical coherence tomography data for the diagnosis of oral cancer in the hamster cheek pouch model. Biomed Opt Express. 2016;7:2000–15.
72. C.A. Patil, H. Krishnamoorthi, D.L. Ellis, T.G. van Leeuwen, A. Mahadevan-Jansen. A clinical probe for combined Raman spectroscopy-optical coherence tomography (RS-OCT) of the skin cancers, 2010, pp. 75480L.
73. García-Hernández A, Roldán-Marín R, Iglesias-Garcia P, Malvehy J. *In Vivo* noninvasive imaging of healthy lower lip mucosa: a correlation study between high-definition optical coherence tomography, reflectance confocal microscopy, and histology. Dermatol Res Pract. 2013;2013:205256.
74. Boppart SA, Oldenburg AL, Xu C, Marks DL. Optical probes and techniques for molecular contrast enhancement in coherence imaging. J Biomed Opt. 2005;10:041208–14.
75. Barton JK, Hoying JB, Sullivan CJ. Use of microbubbles as an optical coherence tomography contrast agent. Acad Radiol. 2002;9:S52–5.
76. Morgner U, Drexler W, Kärtner F, Li X, Pitris C, Ippen E, et al. Spectroscopic optical coherence tomography. Opt Lett. 2000;25:111–3.
77. Rao KD, Choma MA, Yazdanfar S, Rollins AM, Izatt JA. Molecular contrast in optical coherence tomography by use of a pump–probe technique. Opt Lett. 2003;28:340–2.
78. Cang H, Sun T, Li Z-Y, Chen J, Wiley BJ, Xia Y, et al. Gold nanocages as contrast agents for spec-

troscopic optical coherence tomography. Opt Lett. 2005;30:3048–50.
79. Oldenburg AL, Hansen MN, Zweifel DA, Wei A, Boppart SA. Plasmon-resonant gold nanorods as low backscattering albedo contrast agents for optical coherence tomography. Opt Express. 2006;14:6724–38.
80. Agrawal A, Huang S, Wei Haw Lin A, Lee M-H, Barton JK, Drezek RA, Pfefer TJ. Quantitative evaluation of optical coherence tomography signal enhancement with gold nanoshells. J Biomed Opt. 2006;11:041121–8.
81. Wilson R. The use of gold nanoparticles in diagnostics and detection. Chem Soc Rev. 2008;37:2028–45.
82. Kim CS, Wilder-Smith P, Ahn Y-C, Liaw L-HL, Chen Z, Kwon YJ. Enhanced detection of early-stage oral cancer *in vivo* by optical coherence tomography using multimodal delivery of gold nanoparticles. J Biomed Opt. 2009;14:034008.
83. Liba O, SoRelle ED, Sen D, de la Zerda A. Contrast-enhanced optical coherence tomography with picomolar sensitivity for functional in vivo imaging. Sci Rep. 2016;6:23337.